This is the peer-reviewed, final accepted version for American Mineralogist, published by the Mineralogical Society of America.
The published version is subject to change. Cite as Authors (Year) Title. American Mineralogist, in press.
DOI: https://doi.org/10.2138/am-2022-8717. http://www.minsocam.org/

Revision 1

Empirical electronic polarizabilities for use in refractive index measurements at 589.3 nm IV. Hydroxyl polarizabilities

Robert D. Shannon*

Geological Sciences/ CIRES, University of Colorado, Boulder, Colorado 80309

Reinhard X. Fischer

Universität Bremen, FB 5 Geowissenschaften, Klagenfurter Str., D-28359 Bremen (Germany)

C. Van Alsenoy

Department of Chemistry, University of Antwerp, Groenenborgerlaan 171, B-2020 Antwerp, Belgium

ABSTRACT

Refractive indices of minerals and inorganic compounds can be calculated from their chemical compositions using the additivity rule for electronic polarizabilities and converting the sum of polarizabilities α using the Anderson-Eggleton relationship $\alpha_{AE} = \frac{(n_D^2-1)V_m}{4\pi+\left(\frac{4\pi}{3}-2.26\right)(n_D^2-1)}$ with the molar volume V_m solved for the mean refractive index n_D at 589.3 nm. Whereas the polarizability of cations is a single parameter, the polarizability of anions is described by a 2-parameter term $\alpha_- = \alpha_-^o \cdot 10^{-N_o/V_{an}^{1.20}}$ with α_- = anion polarizability, V_{an} = anion molar volume, and the two least-squares parameters α_-^o (corresponding to free-ion polarizability) and N_o. For hydroxyls, Shannon and Fischer (American Mineralogist 101, 2016, 2288-2300) introduced different parameter sets for non-H-bonded hydroxyls (α_-^o=1.79 Å^3, N_o=1.792 Å$^{3.6}$) and moderately strong

This is the peer-reviewed, final accepted version for American Mineralogist, published by the Mineralogical Society of America.
The published version is subject to change. Cite as Authors (Year) Title. American Mineralogist, in press.
DOI: https://doi.org/10.2138/am-2022-8717. http://www.minsocam.org/

H-bonded hydroxyls (α^{o}=1.73 Å^3, N_o=2.042 Å$^{3.6}$). In an effort to understand the lower polarizability of the H-bonded hydroxyl ions, we have evaluated observed and calculated polarizabilities, O–H, H····O, O····O distances, and O–H····O angles in 10 minerals with non-hydrogen-bonded hydroxyls (mean <O····O> distance 3.143 Å, mean <H····O> distance 2.352 Å), in 7 minerals with H-bonded-hydroxyls (<O····O> = 2.739 Å, <H····O> = 1.856 Å), and in 10 minerals with very strongly H-bonded hydroxyls (<O····O> = 2.531 Å, <H····O> = 1.525 Å). On the basis of quantum chemical cluster calculations using atomic parameters of well determined crystal structures of hydroxyl containing compounds, we found that calculated intrinsic polarizabilities of OH are correlated with the hydrogen bond lengths H····O and O····O between donor and acceptor of the H-bond. This is demonstrated for LiOH, brucite ($Mg(OH)_2$), portlandite ($Ca(OH)_2$), clinometaborite (β-HBO_2), sassolite (H_3BO_3), archerite (KH_2PO_4), kalicinite ($KHCO_3$), metaborite (γ-HBO_2), and $NaPO_2(OH)_2$.

Thus, we find that these summed intrinsic polarizabilities for OH-bonds which are involved in H-bonding are significantly lower than the corresponding summed intrinsic polarizabilities for OH-bonds not involved in H-bonding. We attribute the reduction in polarizability of hydroxyl ions in clinometaborite, sassolite, archerite, kalicinite and metaborite, and the compound $NaPO_2(OH)_2$ to the presence of H-bonds and a reduction of Hirshfeld atomic charge on the oxygen atom.

INTRODUCTION

General

Shannon and Fischer (2016) evaluated the dynamic polarizabilities of 2600 minerals and 675 synthetic compounds using refractive indices determined at λ = 589.3 nm (n_D) to yield a unique

This is the peer-reviewed, final accepted version for American Mineralogist, published by the Mineralogical Society of America.
The published version is subject to change. Cite as Authors (Year) Title. American Mineralogist, in press.
DOI: https://doi.org/10.2138/am-2022-8717. http://www.minsocam.org/

set of individual electronic polarizabilities of ions which can be used for the interpretation of optical properties. Various definitions of polarizabilities have been proposed but we use the Anderson-Eggleton relationship (Anderson, 1975; Eggleton, 1991) discussed in Shannon and Fischer (2016) and defined as

$$\alpha_{AE} = \frac{(n_D^2-1)V_m}{4\pi+\left(\frac{4\pi}{3}-c\right)(n_D^2-1)} \quad (1)$$

where α_{AE} = the total polarizability of a mineral or compound, n_D = the refractive index at λ = 589.3 nm, V_m = molar volume in Å^3, and c = 2.26. For example, the total polarizability of albite ($NaAlSi_3O_8$) is calculated according to $\alpha_T(albite) = \alpha_e(Na^+) + \alpha_e(Al^{3+}) + 3\alpha_e(Si^{4+}) + 8\alpha_e(O^{2-})$ using individual polarizabilities, α, given in Shannon and Fischer (2016). The calculated mean values of $<\alpha_{AE}>$ for 54 common minerals and 650 minerals and synthetic compounds differ by less than 3% from the observed values. Using dynamic polarizabilities, we observed systematic deviations in: (1) $M^{2+}SO_4 \cdot nH_2O$, blödite ($Na_2M^{2+}(SO_4)_2 \cdot 4H_2O$), and kieserite-related minerals (Gagné et al. 2018), (2) fast-ion conductors (Shannon et al., 2019), (3) crystal structures containing corner-shared octahedra such as $MTiO_3$ (M = Ca, Sr, Ba), $KNbO_3$, $KTaO_3$, $Ba_{.25}Sr_{.75}Nb_2O_6$ and $KTiOPO_4$, and (4) crystal structures containing edge-shared Fe^{3+}, Mn^{3+}, Ti^{4+}, Mo^{6+}, and W^{6+} octahedra such as $MnWO_4$ (hübnerite) (Shannon and Fischer, 2016).

Hydrogen-bonded minerals and compounds

Included in the data set are 650 non-hydrogen-bonded hydroxyl-containing compounds, ~300 moderately strong hydrogen-bonded hydroxyl-containing compounds, and 35 minerals with very strong H-bonded hydroxyls. Anion polarizabilities are given by

$$\alpha_{-} = \alpha_{-}^{o} \cdot 10^{-N_o/V_{an}^{1.20}} \quad (2)$$

with α_- = anion polarizability, α^o_- = free-ion polarizability, and V_{an} = anion molar volume. Polarizability values for OH^- of 1.79 Å^3, N_o = 1.792 Å$^{3.6}$ [1] allowed a good fit for the calculated vs. observed polarizabilities of the compounds with non-H-bonded hydroxyls. However, compounds with moderately strong H-bonded hydroxyls with O····O distances between 2.6 and 2.9 Å required use of α^o_- (OH^-) = 1.73 Å^3, N_o = 2.042 A$^{3.6}$. In Shannon and Fischer (2006) and Shannon and Fischer (2016), it was believed that when the hydroxyl is very strongly H-bonded, such as in cubic HBO_2 (metaborite), AlOOH (diaspore), $NaCa_2Si_3O_8(OH)$ (pectolite), $CaHPO_4$ (monetite), and KH_2AsO_4, using $\alpha°$ (OH^-) = 1.79 Å^3, N_o = 1.792 Å$^{3.6}$ resulted in a better fit. However, as the calculations in this paper show, the hydroxyl ions in minerals with very strong H-bonded hydroxyls have approximately the same polarizabilities as hydroxyl ions in minerals with moderately strong H-bonded hydroxyls.

There are ~35 structures in the data set that contain very strongly bonded hydroxyl ions defined here by O····O distances less than ~<2.6 Å> in an O—H····O configuration. Wiedemann (1976) showed that very strongly bonded hydroxyls behave differently from moderately H-bonded hydroxyls. It is possible that the different values of very strong and moderate H-bonds result from the tendency of the very strong H-bonds to be more symmetrical (straight O-H…O = 180˚) whereas moderate H-bonds are bent (O-H…O < 180˚). Wiedemann (1976) showed that the polarizability goes up as the O-H…O angle approaches 180 ˚.

In this paper, we seek to understand the origin of the two different OH- polarizabilities in minerals with (1) non-H-bonded hydroxyls [O····O distances > 2.90 Å], and (2) H-bonded

[1] N_o was introduced by Shannon and Fischer (2016) as a dimensionless parameter but formally it has the dimension Å$^{3.6}$ to yield a dimensionless exponent $N_o/V_{an}^{1.20}$ in the equation $\alpha_- = \alpha^o_- \cdot 10^{-N_o/V_{an}^{1.20}}$ considering that V has the dimension Å^3

hydroxyls [O····O distances between 2.6 and 2.9 Å], and very strong H-bonded hydroxyls [O····O distances < 2.60 Å] (Shannon and Fischer, 2016).

DATABASE AND CALCULATIONS

Optically-derived hydroxyl polarizabilities and associated interatomic distances.

Table 1 lists the observed and calculated polarizabilities, O–H, H····O, O····O distances, and O–H····O angles in 10 minerals with non-hydrogen-bonded hydroxyls, in 7 minerals with H-bonded-hydroxyls, and in 10 minerals with very strongly H-bonded hydroxyls and compounds, and associated references. Table 2 summarizes the refractive indices of these minerals and compounds. The refractive indices, polarizabilities, and hydroxyl structure data were taken from studies on well-characterized compounds with accurately known compositions (Shannon et al, 2017). To provide the most accurate hydroxyl distances, neutron diffraction data were used except for sassolite, metaborite, and clinometaborite where X-ray diffraction data were used. Goethite, lepidocrocite, and manganite data were omitted because those structures contain edge-shared octahedra which result in higher than normal total polarizabilities (Shannon and Fischer, 2016).

Cluster calculations for hydroxyl-containing minerals.

We use quantum chemical cluster calculations in a number of model systems. Here we show that the reduction in polarizabilities from refractive index measurements can be related to a reduction in polarizability of the OH bonds in these systems. To this end, polarizabilities calculated quantum chemically at the B3LYP/aug-cc-pVDZ level of theory were partitioned, using the standard Hirshfeld technique (Rousseau et al., 2000), into atomic contributions as

proposed by Krishtal et al. (2006). For our purpose, the most relevant parameter of this partitioning technique is the intrinsic polarizability of a given atom. Using the intrinsic atomic polarizability tensor, the intrinsic polarizability represents the response to the applied electric field (Krishtal et al., 2006). The atomic contributions are obtained by Hirshfeld partitioning in DFT calculations. For further details see, e.g., Krishtal et al. (2006). The intrinsic polarizabilities are directly related to static electronic polarizabilities which can be determined from dispersion curves of refractive indices by extrapolation to infinite wavelength (Shannon and Fischer, 2006). Calculated intrinsic polarizabilities are usually given in atomic units (a.u.) of a_0^3 where a_0 is the Bohr radius 0.5291772083 Å. Consequently, a.u. can be converted with a factor of 0.148184 to $Å^3$ which is the common unit to describe experimentally determined and calculated electronic polarizabilities (Miller, 2022). Since the static polarizabilities of OH show a curve progression similarly to dynamic polarizabilities (but with lower absolute values) as a function of the anion volume, we can compare here the intrinsic polarizabilities of OH calculated from DFT calculations with the dynamic electronic polarizabilities of OH determined from equ. (2) with parameters from Shannon and Fischer (2016). This is shown in Figure 1 where hydroxyl polarizabilities are plotted vs. anion volume. The green curve represents static polarizabilities with parameters from Shannon and Fischer (2006), and the blue and red curves represent dynamic polarizabilities at 589.3 nm with parameter sets 1.79 $Å^3$, 1.792 $Å^{3.6}$ for non-H-bonded OH (blue) and 1.73 $Å^3$, 2.042 $Å^{3.6}$ for H-bonded OH (red) (see the section on hydrogen-bonded minerals and compounds for details). The intrinsic polarizability summed over the two atoms constituting a given OH bond is compared for a number of OH bonds in the modelled minerals.

In cluster calculations, effects of bulk interactions in the crystal are not taken into account and, as such, through considering only specific interactions between two neighboring clusters,

allows us to compare the partitioned intrinsic polarizabilities of H-bonded with non-H-bonded hydroxyls.

Partitioning of polarizabilities leads to atomic intrinsic polarizabilities. Summing the atomic intrinsic polarizabilities for an O and H atom making up an OH-bond, gives intrinsic polarizabilities for a OH-bond. In all of our model calculations, we used the crystallographic coordinates of the clusters from the literature and transformed them into cartesian reference systems. For archerite (KH_2PO_4) for instance, a dimer was constructed containing two KH_2PO_4 clusters. We compared the summed atomic intrinsic polarizabilities of the O and H atoms which make up the different OH-bonds in these clusters and found that these summed intrinsic polarizabilities for OH-bonds which are involved in H-bonding are lower than the corresponding summed intrinsic polarizabilities for OH-bonds not involved in H-bonding.

RESULTS AND DISCUSSION

Optically-derived hydroxyl polarizabilities and associated interatomic distances in hydroxyl minerals

Table 3 shows a summary of O–H, H····O, O····O distances, and O–H····O angles with mean values of the <O–H>, <H····O>, <O····O> distances and the <O–H····O> angles. These values are in general agreement with corresponding values from Jeffrey (1997) in his generalization of bond distances in hydrogen-bonded compounds and with values from Joswig et al. (1982) for 23 compounds with very strong hydrogen bonds studied by neutron diffraction. There are some apparent outliers in the Joswig et al. (1982) data: [1-phenyl-1,3-butanedione, imidazole H maleate, $LiHC_8H_4O_4.CH_3OH$ and Ni ($C_{13}H_{21}N_5O_4$)].

This is the peer-reviewed, final accepted version for American Mineralogist, published by the Mineralogical Society of America.
The published version is subject to change. Cite as Authors (Year) Title. American Mineralogist, in press.
DOI: https://doi.org/10.2138/am-2022-8717. http://www.minsocam.org/

Figure 2 shows a plot of α(OH) vs H····O distance. Hydroxyl polarizabilities are shown for strongly bonded OH (green), moderately strongly bonded OH (red), and non-bonded OH (blue) as defined by their O····O distances. The figure also shows somewhat more scatter of the very strong (VS)-H-bonded data than the moderately strong H-bonded data.

Shannon and Fischer (2016) found that a polarizability value of 1.79 $Å^3$, N_o = 1.792 $Å^{3.6}$ allows a good fit for the calculated vs. observed polarizabilities of the compounds with non-H-bonded hydroxyls. However, minerals with moderately strong H-bonded hydroxyls with O····O distances between 2.6 Å and 2.9 Å required use of $\alpha°(OH^-)$ = 1.73 $Å^3$, N_o = 2.042 $A^{3.6}$. In Shannon and Fischer (2006, 2016), we had no rationale for the reduction in polarizability for H-bonded hydroxyls. In this paper, we seek the origin of the two different OH- polarizabilities in minerals with (1) non-H-bonded hydroxyls and (2) H-bonded hydroxyls and very strong H-bonded hydroxyls by calculation of the polarizabilities of the non-H-bonded OH in LiOH, brucite ($Mg(OH)_2$), portlandite ($Ca(OH)_2$), the H-bonded OH in sassolite (H_3BO_3) and clinometaborite (β-HBO_2) and the very strong H-bonded OH in metaborite (γ- HBO_2), kalicinite ($KHCO_3$), $NaPO_2(OH)_2$ and archerite (KH_2PO_4).

Hydroxyl polarizability calculations for LiOH, brucite, portlandite, clinometaborite, sassolite, archerite, kalicinite, metaborite, and $NaPO_2(OH)_2$.

Empirically, we have found that compounds with H-bonded OH groups show a better fit with a smaller polarizability. It is desirable to confirm this observation with theoretical calculations. This has already been observed in calculations of H_2O clusters (Senet et al., 2005 and Krishtal et al., 2006). Here we look at brucite, portlandite, clinometaborite,

sassolite, archerite, kalicinite, metaborite, and synthetic LiOH and $NaPO_2(OH)_2$. For these systems, several dimers are considered each of which allows calculation of the effect of H-bonding on the different OH groups in the system in two ways. First, by comparing in the dimer itself OH-polarizabilities of H-bonded with non-H-bonded OH hydroxyls and second by comparing the calculated OH-polarizabilities of these bonds in the dimer with the corresponding values in the monomers. Experimental geometries were used in all calculations.

Brucite ($Mg(OH)_2$), portlandite ($Ca(OH)_2$) and LiOH, in which no H-bonded OH bonds are present, serve as a reference. The intrinsic polarizabilities for the OH bonds in these three systems, respectively, (Table 4) are 6.827 a.u. (brucite), 7.297 a.u. (portlandite) and 7.369 a.u. (LiOH) (a.u. = atomic units). These values were calculated for a single cluster with the experimental geometry.

Clinometaborite

Clinometaborite contains 3-rings formed by a linkage of BO_3, $BO_2(OH)$, and $BO_3(H_2O)$ representing a monomer (in our calculations of intrinsic polarizabilities) with composition $B_3O_4(OH)(H_2O)$. O4 is counted only once as a bridging atom between two monomers as shown in Figure 3. Thus, a monomer has one hydroxyl group (O6-H3) and one H_2O molecule (H1-O5-H2). The unit cell contains 4 such monomers yielding the composition $(B_3O_4(OH)(H_2O))_4$. All three H atoms form hydrogen bonds with neighboring O atoms with distances d(O6-H3⋯O3) = 1.775(8) Å, d(O5-H1⋯O6) = 1.774(8) Å, and d(O5-H2⋯O1) = 1.749(7) Å. In order to calculate the intrinsic polarizabilities of the H-bonded groups, three different dimers were built from the monomers: (1) Two monomers connected via the O5-H1⋯O6 H-bond, (2) two

monomers connected via two O6-H3···O3 H-bonds, and (3) two monomers connected via two O5-H2···O1 H-bonds. In Table 5, the intrinsic polarizabilities α for the dimers and the corresponding monomers are listed where the first three and the last three entries for each of the dimers correspond to a monomer, respectively. The H-bonding configuration is renamed in Table 5 to allow for separate calculations for symmetrically equivalent atoms (see footnote in Table 5). In the first dimer, there is a large reduction in α in comparison with the free monomers for both the OHb bond of the second monomer (-0.888 a.u.) and for the OHs bond of the first monomer (-1.110 a.u.). A smaller reduction (-0.233 a.u.) is noticed for the OHa bond of the second monomer which is probably due to strong interactions between both H-bonds of the H_2O molecule in the second monomer. The difference in α's for the remaining OH bonds is negligible. Similar trends are noticed for the second and third dimer.

Sassolite

For modelling sassolite, a cluster of six $B(OH)_3$ groups was selected to calculate the intrinsic polarizabilities as shown in Figure 4. Three types of H-bonds can be identified. (1) the H-bonds in the inner 6-membered ring (Hi···O in Figure 4), (2) the H-bonds of the outer ring (Ho···O), and (3) non-bonding H-O contacts pointing up from the plane of drawing (Hn-O).This does not represent the situation in an infinite inorganic crystal where the H-bond interactions are symmetrically equivalent but allows comparison of intrinsic polarizabilties of the different hydroxyls in the model. In Table 6, the intrinsic 'inner' cycle (OHi) polarizabilities are compared with those in the 'outer' cycle (OHo) and with the non-H-bonded OH (OHn). The largest decrease in α is noticed for the 'inner' cycle OH (-1.470 a.u). It is remarkable, that the polarizabilities of the non-bonded OH (OHn, -0.845 a.u.) are also reduced from the

corresponding value of OH in the 'outer' cycle (OHo, -0.533 a.u.). This seems to be a more general trend already noticed in clinometaborite and which will be described in archerite where the polarizabilities of OH with H-bonding were also significantly reduced.

Kalicinite

In kalicinite ($KHCO_3$), four types of H-bonds linking two $KHCO_3$ clusters, each containing one H-bond, are present. The respective bond lengths are: 1.587 Å, 2.759 Å, 3.385 Å, and 3.417 Å. As before, the effect of these H-bonds on hydroxyl polarizabilities is modelled using dimers. The first planar dimer contains the two shortest H-bond interactions, 1.587 Å and 2.759 Å. In the second dimer, two H-bonds of 3.385A closing a six membered ring where the two HCO_3^- units are in a parallel arrangement. In the asymmetric third dimer, the OH in one monomer forms H-bonding to the OH in the second monomer with a distance of 3.417 Å. In this dimer, both HCO_3^- units are in a displaced, parallel orientation, with an O-H···O angle of 99.07°. Table 7 lists the calculated polarizabilities. H-bonded OH's show a consistently lower calculated α in comparison with the monomer. In particular, in dimer 1, a reduction of -1.136 a.u. is noticed. In dimer 2, the reduction in α is smaller, probably because the H-bond is longer than 3 Å. Also, in the third dimer, the H-bonded OH has a lower α (4.206 Å) than the non-H-bonded OH (4.800 Å) which is comparable to the free monomer polarizability. Here again, the reduction is smaller, probably because the H-bonded distance is larger than 3 Å.

Archerite

For archerite (KH_2PO_4), a dimer is constructed containing all three H-bond interactions. The respective H-bond distances are 1.429 Å, 2.640 Å, and 3.456 Å (Nelmes et al., 1982). Figure 5

248 shows the atomic configuration used in the model. In the KH_2PO_4-dimer used in this study, the
249 effect of H-bonding on the OH polarizability is shown. Only the PO_4-units are drawn with K-
250 atoms omitted. Polarizabilities of the different OH's in the dimer are listed in Table 8 and the
251 structure projection is shown in Figure 5. Each monomer contains two OH's. The first two H-
252 bonding distances belong to the first monomer, the last two belong to the second monomer. The
253 largest reduction (-1.843) is noticed for the OH participating in the H-bond of 1.429 Å. This
254 bond actually occurs in all three types of H-bonds. A second significant reduction is noticed for
255 the OH belonging to the second monomer (the last entry in Table 8). There is a H-bond
256 interaction between the first and the last OH listed in Table 8. The H-bond distance of 3.456 Å,
257 although large, still has a significant effect. This effect was also observed in clinometaborite.
258
259 **Metaborite**
260 For metaborite, the polarizability was calculated for a single cluster containing 24 B atoms,
261 48 O atoms, and 24 H atoms. The structure contains 24 H-bonds, all with the same bond length
262 of 1.00851 Å. Four types of H-bond interactions are found in this structure with bond lengths:
263 1.479 Å, 2.573 Å, 2.758 Å, and 3.422 Å (Freyhardt et al., 2000). Twelve H-bonds are involved
264 in all four H-bond interactions, twelve H-bonds are only involved in H-bond interactions with
265 bond length 2.573 Å. Here again, intrinsic polarizabilities of the OH's involved in strong H-
266 bonding were calculated as 1.411 a.u. whereas the α's for the other types of H-bonds are
267 calculated as 4.309 a.u. A significant reduction in α is noticed for the strongly H-bonded OH in
268 comparison with the non-H-bonded OH.
269
270

This is the peer-reviewed, final accepted version for American Mineralogist, published by the Mineralogical Society of America.
The published version is subject to change. Cite as Authors (Year) Title. American Mineralogist, in press.
DOI: https://doi.org/10.2138/am-2022-8717. http://www.minsocam.org/

$NaPO_2(OH)_2$

In $NaPO_2(OH)_2$, two types of monomers are present, each containing two OH groups. In one type of monomer, the distances for the O-H bonds are 1.041 Å and 1.026 Å whereas in the other type of monomer the corresponding bond lengths are 1.001 Å and 1.003 Å. A number of H-bonds is present between these monomers. Considering only those H-bonds which are smaller than 2.5 Å, four types of dimers can be identified with H-bond distances 1.458 Å (dimer1), 1.524 Å (dimer2), 1.589 Å (dimer 3) and 1.644 Å (dimer 4). In Table 9, the intrinsic polarizabilities of the OH's in the Na_2HPO_4 dimers are compared with the corresponding monomer values. Since each monomer contains two H-bonds, the first two H-bonds listed in Table 9 belong to the first monomer and the last two to the second monomer. In the first asymmetric dimer, a significant reduction in α is observed for the OH involved in H-bonding (-0.807 a.u.) in comparison to the non-H-bonded OH groups in this dimer. In the remaining three dimers, similar significant reductions in α are observed for OH involved in H-bonding: -0.958 a.u. (dimer 2), -1.181 a.u. (dimer 3), and -1.160 a.u. (dimer 4). As in all previous cases, change in α for OH bonds not involved in H-bonding is small to negligible.

Change of intrinsic polarizability with H-bond distance for the model dimer CH_3OCH_3-CH_3OH

In order to further rationalize the reduction of the intrinsic polarizability parameter upon H-bond formation, the intrinsic polarizability was calculated as a function of the H$\cdots$O nonbonded distance for a model dimer, namely a CH_3OCH_3-CH_3OH dimer. For the CH_3OCH_3-CH_3OH dimer depicted in Figure 6, the relative orientation is similar, a H-bond is formed by the OH-group of methanol to the O atom of dimethylether. The OH bond of

294 methanol lies in the plane formed by the C-O-C atoms of dimethylether. For the dimer,
295 CH_3OCH_3-CH_3OH, the geometry used for the monomers was the optimal one at the level
296 of theory (B3LYP/aug-cc-pVDZ) used in all our calculations. This geometry was kept
297 fixed, only the length of the H-bond was varied. Intrinsic polarizabilities are tabulated as a
298 function of the H····O bond distance in Å. An infinite (∞) distance refers to the intrinsic
299 polarizability for a free monomer. The values for the calculated intrinsic polarizability α as
300 a function of the H····O-distance are given for methanol-dimethylether in Table 10 and
301 Figure 7. There is a continuous reduction in α with decreasing distance between methanol
302 and dimethylether: 0.6 at a typical H-bond distance of 2.0 Å in comparison with the values
303 for the OH polarizability in a free CH_3OH molecule (4.747). The simulation of H-bonding
304 based on varying H····O distances shows that OH polarizability continuously decreases
305 with decreasing H····O distances. These results for methanol-dimethylether should apply
306 equally well to OH in minerals.
307 Libowitzky (1999a,1999b), in a classic study, established the dependence of O-H
308 stretching frequencies on O····O and OH····O hydrogen bond lengths in 65 silicate,
309 oxyhydroxide, carbonate, sulfate, phosphate and arsenate minerals. This dependence
310 (Figures 1 and 2 in Libowitzky 1999a, 1999b), is strikingly similar to the plots of
311 Hirshfeld charge vs. polarizability and Hirshfeld charge vs. O····H distance in methanol-
312 dimethyl ether dependence shown in Figure 7 and suggests a strong correlation between
313 O-H stretching frequencies, Hirshfeld charges, and polarizabilities. However, this
314 correlation could not be made because of insufficient IR data on the minerals in this study.
315
316

317 **Source of the reduction in hydroxyl polarizability**

318 Senet et al. (2005) and Krishtal et al. (2006) studied the effects of hydrogen bonding on the
319 polarizability of water molecules and concluded that the polarizability of intramolecular water is
320 significantly reduced (35%) from the polarizability of an isolated molecule. They attributed the
321 reduction in water polarizability to the presence of H-bonds and a reduction of Hirshfeld atomic
322 charge on the oxygen atom, Rousseau et al. (2000) and Senet et al. (2005, 2006). In our analysis,
323 we see a significant reduction of Hirshfeld charge from LiOH, brucite and portlandite to
324 clinometaborite, sassolite, archerite, kalicinite and metaborite, and the compound $NaPO_2(OH)_2$ in
325 Tables 4-10 and Figure 8, showing that the reduction of hydroxyl polarizability comes from
326 reduction of Hirshfeld charge on the oxygen atom.

327

328 **IMPLICATIONS**

329 We have shown here that the electronic polarizabilities and thus the refractive indices of
330 hydroxides depend on the strengths of the hydrogen bonds as expressed by the OH····O bond
331 lengths. This is verified by quantum chemical cluster calculations and established by the
332 investigation of minerals with non-bonded and H-bonded hydroxyls. It also coincides with the
333 observation by Libowitzky (1999a,1999b) who found strong correlation of IR stretching
334 frequencies and OH····O hydrogen bond lengths in many minerals. So, our study of the
335 dependence of polarizabilities and Hirshfeld charges on O····O and H····O distances adds
336 significantly to that knowledge. The presence of H-bonds in minerals results in a lowering of
337 total electronic polarizabilities and refractive indices. Conversely, these findings can be used to
338 identify the H-bonding character in hydroxide crystals.

339

ACKNOWLEDGEMENTS

We thank Ruth Shannon for tabulation of data, and Frank Hawthorne and an anonymous reviewer for improving the manuscript.

REFERENCES

Anderson, O.L. (1975) Optical properties of rock-forming minerals derived from atomic properties. Fortschritte der Mineralogie, 52, 611–629.

Ashmore, J.P., and Petch, H.E. (1970) Hydrogen positions in potassium pentaborate tetrahydrate by neutron diffraction. Canadian Journal of Physics, 48, 1091-1097.

Bartl, H. (1970) Untersuchung der Wasserstoffbindungen in Zunyit, $Al_{12}(OH,F)_{18}(AlO_4)(Si_5O_{16})Cl$, durch Neutronenbeugung. Neues Jahrbuch für Mineralogie, Monatshefte, 1970, 552-557.

Böggild, O. B. (1915) IX. Ussingit, ein neues Mineral von Kangerdluarsuk. Zeitschrift für Kristallographie, 54, 120-126.

Burns, P.C., and Hawthorne, F.C. (1993) Hydrogen bonding in colemanite: an X-ray and structure-energy study. Canadian Mineralogist, 31, 297-304.

Busing, W.R., and Levy, H.A. (1957) Neutron diffraction study of calcium hydroxide. Journal of Chemical Physics, 26, 563-568.

Busing, W.R., and Levy, H.A. (1958) A single crystal neutron diffraction study of diaspore, AlOOH. Acta Crystallographica, 11, 798-803.

Catti, M., Ferraris, G., and Filhol, A. (1977) Hydrogen bonding in the crystalline state. $CaHPO_4$ (monetite). $P\bar{1}$ or $P1$? A novel neutron diffraction study. Acta Crystallographica, B33, 1223-1229.

Catti, M., Ferraris, G., Hull, S., Pavese, A. (1995) Static compression and H disorder in brucite, $Mg(OH)_2$, to 11 GPa: a powder neutron diffraction study. Physics and Chemistry of Minerals 22, 200-206.

Choudhary, R.N.P., Nelmes, R.J., and Rouse, K.D. (1981) A room-temperature neutron-diffraction study of NaH_2PO_4. Chemical Physics Letters, 78, 102-105.

Christensen, A.N., Ollivier, G. (1972) Hydrothermal preparation and low temperature magnetic properties of $Mn(OH)_2$. Solid State Communications, 10, 609-614.

Christensen, A.N.,Hansen, P., and Lehmann, M.S. (1977) Isotope effects in the bonds of α-CrOOH and α -CrOOD. Journal of Solid State Chemistry, 21, 325-329.

Cook, W.R., and Hubby, L.M. (1976) Indices of refraction of potassium pentaborate. Journal of the Optical Society of America, 66, 72-73.

Craven, B.M., and Sabine, T.M. (1966) A neutron diffraction study of orthoboric acid $D_3{}^{11}BO_3$. Acta Crystallographica, 20, 214-219.

Dachs, H. (1959) Bestimmung der Lage des Wasserstoffs in LiOH durch Neutronenbeugung. Zeitschrift für Kristallographie, 112, 60-67.

Dann, S.E., Mead, P.J., and Weller, M.T. (1996) Löwenstein's rule extended to an aluminium rich framework. The structure of bicchulite, $Ca_8(Al_2SiO_6)_4(OH)_8$, by MAS NMR and neutron diffraction. Inorganic Chemistry, 35, 1427-1428.

Demartin, F., Gramaccioli, C.M., and Campostrini, I. (2011) Clinometaborite, natural β-metaboric acid, from La Fossa crater, Vulcano, Aeolian Islands, Italy. Canadian Mineralogist, 49, 1273-1279.

384 Eggleton, R.A. (1991) Gladstone-Dale constants for the major elements in silicates: Coordination
385 number, polarizability, and the Lorentz-Lorentz relation. Canadian Mineralogist, 29, 525–
386 532.
387 Ernst T. (1933) Darstellung und Kristallstruktur von Lithiumhydroxyd. Zeitschrift für
388 physikalische Chemie, B20, 65-88.
389 Fleischer, M. (1965) New Mineral Names. American Mineralogist, 50, 261-262**.**
390 Freyhardt, C.C., Wiebcke, M., and Felsche, J. (2000) The monoclinic and cubic phases of
391 metaboric acid (precise redeterminations). Acta Crystallographica C56, 276-278.
392 Gagné, O., Hawthorne, F., Shannon, R.D., and Fischer, R.X. (2018) Empirical electronic
393 polarizabilities: deviations from the additivity rule. I. $M^{2+}SO_4 \cdot nH_2O$, blödite
394 $Na_2M^{2+}(SO_4)_2 \cdot 4H_2O$, and kieserite-related minerals with sterically strained structures.
395 Physics and Chemistry of Minerals 45, 303-310.
396 Gatta, G.D., McIntyre, G.J., Bromiley, G., Guastoni, A., and Nestola, F. (2012) A single-crystal
397 neutron diffraction study of hambergite, $Be_2BO_3(OH,F)$. American Mineralogist, 97, 1891-
398 1897.
399 Gatta, G.D., Jacobsen, S.D., Vignola, P., McIntyre, G.J., Guastella, G., and Abate, L.F. (2014)
400 Single-crystal neutron diffraction and Raman spectroscopic study of hydroxylherderite,
401 $CaBePO_4(OH,F)$. Mineralogical Magazine, 78, 723-737.
402 Hainsworth, F.N., and Petch, H.E. (1966) The structural basis of ferroelectricity in colemanite.
403 Canadian Journal of Physics, 44, 3083-3107.
404 Hill, W.L., and Hendricks, S.B. (1936) Composition and properties of superphosphate – calcium
405 phosphate and calcium sulfate constituents as shown by chemical and X-ray diffraction
406 analysis. Industrial and Engineering Chemistry, Analytical Edition, 28, 440–447.

Ingerson, E. and Morey, G. W. (1943) Preparation and properties of some compounds in the system H_2O-Na_2O-P_2O_5. American Mineralogist, 28, 448–455.

Jeffrey, G.A. (1997) An Introduction to Hydrogen Bonding, Chapter 3 Strong hydrogen bonds, Oxford University Press. pp303.

Joswig, W., Fuess, H., and Ferraris, G. (1982) Neutron diffraction study of the hydrogen bond in trisodium hydrogenbissulfate and a survey of very short O-H···O bonds. Acta Crystallographica B38, 2798-2801.

Kennedy, N.S.J., and Nelmes, R.J. (1980) Structural studies of RbH_2PO_4 in its paraelectric and ferroelectric phases. Journal of Physics, C13, 4841-4853.

Khidirov, I., and Om, V.T. (1993) Localization of hydrogen atoms in rare earth metal trihydroxides $R(OH)_3$. Physica Status Solidi, A140, K59-K62.

Koritnig, S. (1962) In: Landolt-Börnstein, Band II. Teil 8. Optische Konstanten (Hellwege, K.H., Hellwege, A.M., Eds.), p. 43-404, Springer-Verlag, Berlin.

Kracek, F.C., Morey, G.W., and Merwin, H.E. (1938) The system, water – boron oxide. American Journal of Science, 35, 143-171.

Krishtal, A., Senet, P., Yang, M., and Van Alsenoy, C. (2006) A Hirshfeld partitioning of polarizabilities of water clusters. Journal of Chemical Physics 125, 034312 1-7.

Leavens, P. B., Dunn, P.J., and Gaines, R. V. (1978) Compositional and refractive index variations of the herderite-hydroxyl-herderite series. American Mineralogist, 63, 913-917.

Levy, H.A., Peterson, S.W., and Simonsen, S.H. (1954) Neutron diffraction study of the ferroelectric modification of potassium dihydrogen phosphate. Physical Review, 93, 1120-1121.

Libowitzky, E. (1999a) Correlations of O-H stretching frequencies and O-H···O hydrogen bond lengths in minerals. Monatshefte für Chemie, 130, 1047–1059.

Libowitzky, E. (1999b) Correlations of O-H stretching frequencies and O-H···O hydrogen bond lengths in minerals. In P. Schuster and W. Mikenda, Eds., Hydrogen Bond Research, p. 103-115. Springer-Verlag Vienna.

Marcopoulos, T., and Economou, M. (1981) Theophrastite, $Ni(OH)_2$, a new mineral from northern Greece. American Mineralogist, 66, 1020-1021.

McClune, W.F. (1989) JCPDS 1989 reference, Powder Diffraction File 1989. JCPDS-International Centre for Diffraction Data, Swarthmore, Pennsylvania, Vol. 27, p.66.

Medenbach, O., and Shannon, R.D. (1997) Refractive indices and optical dispersion of 103 synthetic and mineral oxides and silicates measured by a small-prism technique**.** Journal of the Optical Society of America, B14**,** 3299-3318.

Merwin, H.E. (1930) Refractivity of birefringent crystals. In: International critical tables of numerical data, physics, chemistry and technology Vol. VII (Washburn, E.W., Ed.) McGraw-Hill Book Company, p. 16-33.

Miller, T.M. (2022) Polarizabilities of atoms and molecules in: CRC Handbook of Chemistry and Physics, 102nd Edition (R. Rumble, Ed.) CRC Press Taylor & Francis Group.

Milton, C., Appleman, D.E., Appleman, M.H., Chao, E. C. T., Cuttitta, F., Dinnin, J.I., Dwornik, E.J., Ingram, B.L., and Rose, H. J. (1976) Merumite - A Complex Assemblage of Chromium Minerals from Guyana. Geological Survey Professional Paper 887, United States Government Printing Office, Washington 1-29.

Nelmes, R.J., Meyer, G.M., and Tibballs, J.E. (1982) The crystal structure of tetragonal KH_2PO_4 and KD_2PO_4 as a function of temperature. Journal of Physics, C15, 59-75.

Ohashi, Y., and Finger, L.W. (1978) The role of octahedral cations in pyroxenoid crystal chemistry. I. Bustamite, wollastonite, and the pectolite-schizolite-serandite series. American Mineralogist, 63, 274-288.

Palache, C., Berman, H., and Frondel, C. (1944) Dana's System of Mineralogy, 7th ed., v. I Elements, sulfides, sulfosalts, oxides, 834 pp. Wiley. p. 639.

Rossi, G., Tazzoli, V., and Ungaretti, L. (1974) The crystal structure of ussingite. American Mineralogist, 59, 335-340.

Rousseau, B., Peeters, A., and Van Alsenoy, C. (2000) Systematic study of the parameters determining stockholder charges. Chemical Physics Letters 324, 189–194.

Roy, R. and McKinstry, H.A. (1953) Concerning the so-called $Y(OH)_3$-type structure and the structure of $La(OH)_3$. Acta Crystallographica, 6, 365-366.

Schaller, W.T. (1955) The pectolite-schizolite-serandite series. American Mineralogist, 40, 1022–1031.

Schröder, A., and Hoffmann, W. (1956) Zur Optik des Colemanits. Neues Jahrbuch für Mineralogie. Monatshefte, 1956, 265-271.

Senet, P., Yang, M., Delarue, P., Lagrange, S., and Van Alsenoy, C. (2005) Understanding Local Dielectric Properties of Water Clusters. Lecture Series on Computer and Computational Science, 3, 234-247.

Senet, P., Yang, M., and Van Alsenoy, C. (2006) Charge distribution and polarisabilities of water clusters. In "Atoms, Molecules and Clusters in Electric Fields. Theoretical Approaches to the Calculation of Electric Polarizability. George Maroulis Ed., Computational, Numerical and Mathematical Methods in Sciences and Engineering - Vol. 1, pp. 657-679, Imperial College Press.

475 Shannon, R.D., and Fischer, R.X. (2006) Empirical electronic polarizabilities in oxides,
476 hydroxides, oxyfluorides, and oxychlorides. Physical Review B73, 235111 1-28.
477 Shannon RD, and Fischer RX (2016) Empirical electronic polarizabilities of ions for the
478 prediction and interpretation of refractive indices: Oxides and oxysalts. American Mineralo-
479 gist, 101, 2288–2300.
480 Shannon, R.D., Shannon, R.C., Medenbach, O., and Fischer, R.X. (2002) Refractive index and
481 dispersion of fluorides and oxides. Journal of Physical and Chemical Reference Data, 31,
482 931-970.
483 Shannon R.D., Kabanova, N.A., and Fischer, R.X. (2019) Empirical electronic polarizabilities:
484 Deviations from the additivity rule. II. Structures exhibiting ion conductivity. Crystal
485 Research and Technology 54, 1900037, 1-11.
486 Shannon, R.C., Lafuente, B., Shannon, R.D., Downs, R.T., and Fischer, R.X. (2017) Refractive
487 indices of minerals and synthetic compounds. American Mineralogist, 102, 1906–1914.
488 Shannon, R.D., Subramanian, M.A., Mariano, A.N., Gier, T.E., and Rossman, G.R. (1992)
489 Dielectric constants of diaspore and B-, Be-, and P-containing minerals, the polarizabilities
490 of B_2O_3 and P_2O_5, and the oxide additivity rule. American Mineralogist, 77, 101-106.
491 Szytula, A., Murasik, A., and Balanda, M. (1971) Neutron diffraction study of $Ni(OH)_2$. Physica
492 Status Solidi, B43, 125-128.
493 Thomas, J.O., Tellgren, R., and Olovsson, I. (1974) Hydrogen bond studies. XCII. Disorder in
494 $(HCO_3)^{2-}{}_2$ and $(DCO_3)^{2-}{}_2$ dimers: a neutron diffraction study of $KHCO_3$ and $KDCO_3$. Acta
495 Crystallographica, B30, 2540-2549.
496 Tilley, C.E. (1933) Portlandite, a new mineral from Scawt Hill, Co. Antrim. Mineralogical
497 Magazine, 23, 419-420.

Turco, G. (1962) La zunyite: recherches expérimentales physico-chemiques en liaison avec l'étude du nouveau gisement de Beni-Embarek. Bulletin de la Societe Francaise de Minéralogie et de Cristallographie, 85, 407-458.

Vasilevskya, A.S., Koldobsk, M.F., Lomova, L.G., Popova, V.P., Regulska, T.A., Rez, I.S., Sobesski, Y.P., Sonin A.S., and Suvorov, V.S. (1967) Some physical properties of rubidium dihydrogen phosphate single crystals. Soviet Physics Crystallography, USSR, 12, 383-385.

Vilminot, S., Richard-Plouet, M., André, G., Swierczynski, D., Guillot, M., Bourée-Vigneron, F., and Drillon, M. (2003) Magnetic structure and properties of $Cu_3(OH)_4SO_4$ made of triple chains of spins s = 1/2. Journal of Solid State Chemistry, 170, 255-264.

Vilminot, S., Richard-Plouet, M., André, G., Swierczynski, D., Bourée-Vigneron, F., and Kurmoo, M. (2006) Nuclear and magnetic structures and magnetic properties of synthetic brochantite, $Cu_4(OH)_6SO_4$. Dalton Transactions 2006, 1455-1462.

Wiedemann, E. G. (1976) Model studies on proton correlations in hydrogen bonds. In: The Hydrogen Bond, Vol. I: Theory, Chapter 5. (Eds.: Schuster, P., Zundel, G., Sandorfy, C.) North Holland Publ. Co, pp 245-294.

Williams, E.R., and Weller, M.T. (2012) A variable-temperature neutron diffraction study of ussingite; a strong asymmetric hydrogen bond in an aluminosilicate framework. Physics and Chemistry of Minerals, 39, 471-478.

Williams, E.R., and Weller, M.T. (2014) A variable-temperature neutron diffraction study of serandite: A Mn-silicate framework with a very strong, two-proton site, hydrogen bond. American Mineralogist, 99, 1755-1760.

Winchell, A.N. (1931) The Microscopic Characters of Artificial Inorganic Solid Substances or Artificial Minerals, 2nd ed. Wiley, New York, p. 228.

521 Zachariasen, W.H. (1954) The precise structure of orthoboric acid. Acta Crystallographica, 7,
522 305-310.
523 Zernike, F. (1964) Refractive indices of ammonium dihydrogen phosphate and potassium
524 dihydrogen phosphate between 2000 Å and 1.5 μ. Journal of the Optical Society of America,
525 54, 1215-1220.
526

Figure Captions

Figure 1. Comparison of static and dynamic electronic polarizabilities of hydroxyls

Figure 2. α(OH) vs. H···O distance. α(OH) calculated using 1.79/1.792 for non-bonded OH and using 1.73/2.042 for H-bonded and VS H-bonded OH's.

Figure 3. Crystal-structure projection of clinometaborite showing two monomers linked by the bridging O4 atom according to Figure 2 in Demartin et al. (2011).

Figure 4. Sassolite $B(OH)_3$ group. Hi: OH-bonds in the inner 12-membered ring closed by H-bonds; Ho: OH-bonds of the outermost 24-membered ring system; Hn: OH-bonds not involved in H-bonding.

Figure 5. The KH_2PO_4-dimer used in this study. Only the PO_4-units are drawn, K-atoms have been omitted. H atoms are colored white, oxygen atoms red, phosphorous atoms brown. The H-bonds in this dimer are represented by dashed lines. Ha = OH involved in H-bonding; Hb, Hc, and Hd: terminal H's, not involved in H-bonding.

Figure 6. Methanol-dimethylether-dimer. H atoms are colored white, oxygen atoms red and carbon atoms grey. The H-bond in this dimer is represented by a dashed line.

Figure 7. Hirshfeld charge vs α and H···O distance in methanol-dimethyl ether.

550 **Figure 8**. Comparison of polarizability values derived from refractive index, calculated intrinsic
551 polarizability and Hirshfeld charge on oxygen atom for minerals in this study. Alpha values refer
552 to the left axis and Hirshfeld charge to the right axis.

This is the peer-reviewed, final accepted version for American Mineralogist, published by the Mineralogical Society of America.
The published version is subject to change. Cite as Authors (Year) Title. American Mineralogist, in press.
DOI: https://doi.org/10.2138/am-2022-8717. http://www.minsocam.org/

553 **Table 1**. Chemical composition, total electronic polarizabilities of minerals with H-bonded and non-H-bonded hydroxyls, associated

554 interatomic distances, and references for crystal-structure data.

mineral / compound [a]	chemical composition used for calculating α(calc)	α(obs) (Å^3)	α(calc) (Å^3)	Δ(%)[b]	d(O–H) (Å)	d(H···O) (Å)	d(O···O) (Å)	O–H···O (°)	ref. struct. [f]
non H-bonded									
LiOH	LiOH	2.105	2.097	0.4	0.924	3.053	3.657	124.5	1
brucite	$Mg(OH)_2$	3.911	3.857	1.4	0.919	2.523	3.229	133.9	2
portlandite	$Ca(OH)_2$	5.174	5.102	1.4	0.942	2.665	3.333	128.9	3
pyrochroite	$Mn(OH)_2$	5.340	5.321	0.4	1.040	2.468	3.226	129.0	4
theophrastite	$Ni(OH)_2$	4.935	4.897	0.8	1.065	2.251	3.01	126.6	5
$La(OH)_3$	$La(OH)_3$	8.847	8.945	-1.1	0.811	2.53	2.99	117.3	6
hydroxylherderite	$CaBe(PO_4)(OH)_{0.86}F_{0.14}$)	9.381	9.520	-1.5	0.996	2.544	3.163	124.4	7
antlerite	$Cu_3(OH)_4SO_4$	18.949	19.292	-1.8	0.955	2.474	3.186	131	8
					0.962	2.481	3.220	133	
					0.963	2.183	2.973	138	
bicchulite	$Ca_2(Al_2SiO_6)(OH)_2$	18.046	17.847	1.1	0.936	2.23	3.042	144.6	9
brochantite [c]	$Cu_4(OH)_6SO_4$	24.177	24.534	-1.5	0.883	2.41	2.69	165	10
					0.891	2.07	2.87	149	
					0.954	1.93	2.92	168	
					0.989	2.14	2.98	132	
					0.990	1.88	3.02	148	
					0.999	2.07	3.28	154	
H-bonded									
clinometaborite	$B_3O_4OH \cdot H_2O$	9.429	9.618	-2.0	0.892	1.774	2.658	170.28	11
					0.917	1.775	2.682	170.13	
					0.952	1.749	2.687	167.45	
sassolite	$B(OD)_3$	[d]	[d]	0.1	0.986	1.741	2.727	178.3	12

This is the peer-reviewed, final accepted version for American Mineralogist, published by the Mineralogical Society of America.
The published version is subject to change. Cite as Authors (Year) Title. American Mineralogist, in press.
DOI: https://doi.org/10.2138/am-2022-8717. http://www.minsocam.org/

					0.966	1.724	2.69	180	
					0.951	1.738	2.69	180	
					0.946	1.78	2.724	175.5	
					1.004	1.716	2.704	167	
					0.980	1.766	2.745	178.8	
sassolite	$B(OH)_3$	4.794	4.769	0.5	0.828	1.906	2.727	170.8	13
					0.964	1.756	2.713	171.0	
					0.913	1.806	2.715	173.3	
					0.827	1.895	2.722	177.6	
					0.804	1.933	2.734	173.8	
hambergite	$Be_2(BO_3)(OH)_{0.95}F_{0.05}$	6.513	6.508	0.1	0.971	1.983	2.904	157.5	14
santite	$K(B_5O_6(OH)_4) \cdot 2H_2O$	20.824	21.025	-1.0	0.983	1.892	2.873	176.4	15
					0.926	1.924	2.844	171.8	
					0.980	1.706	2.666	165.6	
					0.949	1.74	2.610	150.9	
colemanite [e]	$CaB_3O_4(OH)_3 \cdot H_2O$	13.970	14.097	-0.9	1.022	2.206	3.063	140.3	16
					0.93	2.229	2.807	119.6	
					0.990	1.776	2.759	171.8	
					0.965	1.773	2.732	171.7	
zunyite	$Al_{13.3}Si_{4.69}Ti_{0.13}P_{0.12}O_{20}(OH)_{14.29}F_{3.59}Cl_{0.96}$	66.935	66.462	0.7	0.990	1.84	2.796		17
					0.989	2.73			
very strong H-bonds									
metaborite	$B_{0.95}Mg_{0.05}OOH$	3.019	3.017	0.1	1.009	1.479	2.485	175.5	18
diaspore	$Al_{0.99}Fe_{0.01}OOH$	3.562	3.461	2.8	0.990	1.694	2.650	160.9	19
grimaldiite	CrOOH	6.076	6.064	0.2	0.878	1.567	2.47	180	20
kalicinite	KCO_2OH	6.122	6.143	-0.4	0.975	1.617	2.587	172.6	21
					1.005	1.587	2.587	173.0	

This is the peer-reviewed, final accepted version for American Mineralogist, published by the Mineralogical Society of America.
The published version is subject to change. Cite as Authors (Year) Title. American Mineralogist, in press.
DOI: https://doi.org/10.2138/am-2022-8717. http://www.minsocam.org/

serandite	$Na_{0.854}K_{0.02}Ca_{0.668}Mn_{1.466}Fe_{0.067}Mg_{0.01}Al_{0.02}Si_{2.91}O_8OH$	19.719	19.890	-0.9	0.990	1.469	2.414	157.4	22
					1.033	1.415	2.414	160.8	
ussingite	$Na_{1.81}K_{0.05}Ca_{0.02}(AlSi_3O_8)(OH)$	17.309	17.110	1.2	1.070	1.412	2.481	176.0	23
$NaPO_2(OH)_2$	$NaPO_2(OH)_2$	7.039	6.845	2.8	1.001	1.644	2.644	177.0	24
					1.003	1.59	2.591	175.6	
					1.026	1.524	2.550	177.6	
					1.040	1.459	2.485	167.7	
archerite	$KPO_2(OH)_2$	8.011	7.833	2.2	1.052	1.437	2.487	180.0	25
$RbPO_2(OH)_2$	$RbPO_2(OH)_2$	8.738	8.513	2.6	1.040	1.459	2.498	177.2	26
monetite	$CaPO_3OH$	7.923	7.945	-0.3	1.042	1.521	2.560	175.6	27
					1.057	1.515	2.658	145.5	
					1.027	1.529	2.459	180.0	

[a] non-hydrogen bonded d(O····O) > 2.9 Å; moderately strong hydrogen bonds d(O····O) 2.6 Å – 2.9 Å; very strong hydrogen bonds d(O····O)<2.6 Å.

[b] α(obs) - α(calc)/ α(obs)

[c] 4 OH are non-bonded, 2 OH are H-bonded

[d] Optical data not determined for this compound

[e] 1.5 OH is non-bonded, 2.5 are H-bonded

[f] References: (1) Dachs (1959); (2) Catti et al. (1995); (3) Busing & Levy (1957); (4) Christensen & Ollivier (1972); (5) Szytula et al. (1971); (6) Khidirov & Om (1993); (7) Gatta et al. (2014); (8) Vilminot et al. (2003); (9) Dann et al. (1996); (10) Vilminot et al. (2006); (11) Demartin et al. (2011); (12) Craven & Sabine (1966); (13) Zachariasen (1954); (14) Gatta et al. (2012); (15) Ashmore & Petch (1970); (16) Hainsworth & Petch (1966); (17) Bartl (1970); (18) Freyhardt et al. (2000); (19) Busing & Levy (1958); (20)

565 Christensen et al. (1977); (21) Thomas et al. (1974); (22) Williams & Weller (2014); (23) Williams & Weller (2012); (24) Choudhary
566 et al. (1981); (25) Levy & Peterson (1954); (26) Kennedy & Nelmes (1980); (27) Catti et al. (1977)
567

568 **Table 2**. Refractive indices, molar volume V_m, anion volume V_{an}, and associated references

mineral / compound	chemical composition	n_x	n_y	n_z	<n>	V_m (Å^3)	V_{an} (Å^3)	ref. RI [a]	ref. V_m [a]
no H-bonds									
LiOH	$LiOH$	1.4639	1.4639	1.4518	1.4599	27.29	27.29	1	1
brucite	$Mg(OH)_2$	1.5665	1.5665	1.5853	1.5728	40.90	20.45	2	3
portlandite	$Ca(OH)_2$	1.575	1.575	1.547	1.5657	54.78	27.39	4	4
pyrochroite	$Mn(OH)_2$	1.723	1.723	1.681	1.7090	45.24	22.62	5	5
theophrastite	$Ni(OH)_2$	1.759	1.759	1.760	1.7593	39.12	19.56	6	6
$La(OH)_3$	$La(OH)_3$	1.740	1.740	1.768	1.7493	71.03	23.68	7	7
hydroxylherderite	$CaBe(PO_4)(OH)_{0.86}F_{0.14})$	1.6090	1.6270	1.6380	1.6247	90.00	18.00	8	9
antlerite	$Cu_3(OH)_4SO_4$	1.7300	1.7370	1.7850	1.7507	151.87	18.98	2	10
bicchulite	$Ca_2(Al_2SiO_6)(OH)_2$	1.6280	1.6280	1.6280	1.6280	172.21	21.52	11	11
brochantite	$Cu_4(OH)_6SO_4$	1.7280	1.7710	1.8000	1.7663	189.95	18.95	12	12
H-bonds									
clinometaborite	$B_3O_4OH \cdot H_2O$	1.4340	1.5700	1.5880	1.5307	106.42	16.51	13	13
sassolite	$B(OD)_3$	1.3370	1.4610	1.4620	1.4200	68.52	22.84	14	15
hambergite	$Be_2(BO_3)(OH)_{0.95}F_{0.05}$	1.5546	1.5886	1.6285	1.5906	66.06	16.51	16	17
santite	$K(B_5O_6(OH)_4) \cdot 2H_2O$	1.4211	1.4336	1.4863	1.4470	279.40	23.28	18	19
colemanite	$CaB_3O_4(OH)_3 \cdot H_2O$	1.5861	1.5919	1.6139	1.5973	140.10	17.51	20	21
zunyite	$Al_{13.3}Si_{4.69}Ti_{0.13}P_{0.12}O_{20}(OH)_{14.29}F_{3.59}Cl_{0.96}$	1.5940	1.5940	1.5940	1.5940	675.00	17.38	22	22
very strong H-bonds									
metaborite	$B_{0.95}Mg_{0.05}OOH$	1.6180	1.6180	1.6180	1.6180	29.27	14.63	23	23
diaspore	$Al_{0.99}Fe_{0.01}OOH$	1.7028	1.7233	1.7503	1.7255	29.51	14.75	16	17
grimaldiite	$CrOOH$	2.1550	2.1550	1.9750	2.0950	34.25	17.12	24	24
kalicinite	KCO_2OH	1.3800	1.4820	1.5730	1.4780	76.70	25.57	25	26
serandite	$Na_{0.854}K_{0.02}Ca_{0.668}Mn_{1.466}Fe_{0.067}Mg_{0.01}Al_{0.02}Si_{2.91}O_8OH$	1.6600	1.6640	1.6880	1.6707	176.38	19.60	27	28
ussingite	$Na_{1.81}K_{0.05}Ca_{0.02}(AlSi_3O_8)(OH)$	1.5037	1.5082	1.5454	1.5191	199.72	22.19	29	30

This is the peer-reviewed, final accepted version for American Mineralogist, published by the Mineralogical Society of America.
The published version is subject to change. Cite as Authors (Year) Title. American Mineralogist, in press.
DOI: https://doi.org/10.2138/am-2022-8717. http://www.minsocam.org/

$NaPO_2(OH)_2$	$NaPO_2(OH)_2$	1.4810	1.5070	1.5170	1.5017	84.06	21.01	31	32
archerite	$KPO_2(OH)_2$	1.5093	1.5093	1.4682	1.4956	96.85	24.21	33	34
$RbPO_2(OH)_2$	$RbPO_2(OH)_2$	1.5054	1.5054	1.4764	1.4957	105.60	26.40	35	36
monetite	$CaPO_3OH$	1.5870	1.6150	1.6400	1.6140	77.32	19.33	37	38

[a] References: (1) Ernst (1933); (2) Koritnig (1962); (3) Shannon et al. (2002); (4) Tilley (1933); (5) Palache et al. (1944); (6) Marcopoulos & Economou (1981); (7) Roy & McKinstry (1953); (8) Leavens et al. (1978); (9) Gatta et al. (2014); (10) Vilminot et al. (2003); (11) McClune (1989); (12) Winchell (1931); (13) Demartin et al. (2011); (14) Kracek et al. (1938); (15) Zachariasen (1954); (16) Medenbach & Shannon (1997); (17) Shannon et al. (1992); (18) Cook & Hubby (1976); (19) Ashmore & Petch (1970); (20) Schröder & Hoffmann (1956); (21) Burns & Hawthorne (1993); (22) Turco (1962); (23) Fleischer (1965); (24) Milton et al. (1976); (25) Merwin (1930); (26) Thomas et al. (1974); (27) Schaller (1955); (28) Ohashi & Finger (1978); (29) Böggild (1915); (30) Rossi et al. (1974); (31) Ingerson & Morey (1943); (32) Choudhary et al. (1981); (33) Zernike (1964); (34) Nelmes et al. (1982); (35) Vasilevskya et al. (1967); (36) Kennedy & Nelmes (1980); (37) Hill & Hendricks (1936); (38) Catti et al. (1977).

This is the peer-reviewed, final accepted version for American Mineralogist, published by the Mineralogical Society of America.
The published version is subject to change. Cite as Authors (Year) Title. American Mineralogist, in press.
DOI: https://doi.org/10.2138/am-2022-8717. http://www.minsocam.org/

578 **Table 3**: Summary of O–H, H····O, O····O distances, and O–H····O angles in hydroxyl minerals and compounds.

O–H (Å)	<O–H> (Å)	H····O (Å)	<H····O> (Å)	O····O (Å)	<O····O> (Å)	O–H····O (˚)	<O–H····O> (˚)
no H-bonds							
0.81-1.07	0.967	1.88-3.05	2.352	2.92-3.66	3.143	117.3-168.0	135.8
		[2.2-3.2]		[3.2-4.0]		[90-150]	
H-bonds							
0.80-1.07	0.936	1.71-2.41	1.856	2.61-2.90	2.739	119.6-180.0	168.1
		[1.5-2.2]		[2.5-3.2]		[130-180]	
very strong H-bonds							
0.88-1.07	1.014	1.41-1.69	1.525	2.41-2.66	2.531	145.5-180.0	171.3
(1.0-1.2)		[1.2-1.5]		[2.2-2.5]		[175-180]	
		(1.2-1.5)		(2.4-2.5)		(153-179)	

579 *Note*: Assignment of bonding character after Shannon and Fischer (2016) with O····O distances non-hydrogen bonded > 2.90 Å,
580 moderately strong H-bonds 2.60-2.90 Å, and O····O very strong H-bonds < 2.60 Å. Values in brackets from Jeffrey (1997), values in
581 parentheses from Joswig et al. (1982).

This is the peer-reviewed, final accepted version for American Mineralogist, published by the Mineralogical Society of America.
The published version is subject to change. Cite as Authors (Year) Title. American Mineralogist, in press.
DOI: https://doi.org/10.2138/am-2022-8717. http://www.minsocam.org/

582 **Table 4**: Comparison of the hydrogen-oxygen bonds in LiOH, brucite, and portlandite.
583 Intrinsic polarizabilities, alpha; Hirshfeld charges on the OH-group
584 (in electron); and bonded OH (hydroxyl) distances d(O-H) as well as non-bonded OH
585 distances d (O… H)**.**
586

	α (a.u.)	charge	d(O-H) (Å)	d(H⋯O) (Å)
LiOH	7.369	-0.544	0.924	3.053
portlandite	7.297	-0.453	0.942	2.665
brucite	6.827	-0.386	0.919	2.523

587
588
589 **Table 5**: Comparison of the OH bond intrinsic polarizabilities between the dimer (α) and
590 corresponding monomers (α_0), together with their difference (α-α_0), the Hirshfeld charge
591 (in electron), bonded OH distance d(OH), H-bonded distance d(H⋯O) and H-bonded
592 valence angle O-H⋯O for the three dimers modelling clinometaborite.

dimer 1	α (a.u.)	α_0 (a.u.)	α - α_0 (a.u.)	charge	d(OH) (Å)	d(H⋯O) (Å)	O-H⋯O (°)
OH2a	3.031	3.101	-0.069	+0.159	0.892		
OH2b	2.958	3.007	-0.049	+0.169	0.952		
OH2s	3.155	4.265	-1.110	-0.011	0.917		
OH1b	2.213	3.101	-0.888	+0.071	0.892	1.774	170.3
OH1a	2.774	3.007	-0.233	+0.137	0.952		
OH1s	4.235	4.265	-0.030	-0.078	0.917		

593
594
595

dimer 2	α (a.u.)	α_0	α - α_0	charge	d(OH)	d(H⋯O)	O-H⋯O

This is the peer-reviewed, final accepted version for American Mineralogist, published by the Mineralogical Society of America.
The published version is subject to change. Cite as Authors (Year) Title. American Mineralogist, in press.
DOI: https://doi.org/10.2138/am-2022-8717. http://www.minsocam.org/

		(a.u.)	(a.u.)		(Å)	(Å)	(°)
OH1a	2.947	3.101	-0.154	+0.155	0.892		
OH1b	2.958	3.007	-0.049	+0.166	0.952		
OH1s	3.338	4.265	-0.927	-0.143	0.917	1.775	170.1
OH2a	2.947	3.101	-0.154	+0.158	0.892		
OH2b	2.958	3.007	-0.049	+0.166	0.952		
OH2s	3.338	4.265	-0.927	-0.139	0.917	1.775	170.1

dimer 3	α (a.u.)	α_0 (a.u.)	α - α_0 (a.u.)	charge	d(OH) (Å)	d(H···O) (Å)	O-H···O (°)
OH1a	2.510	3.101	-0.591	+0.126	0.892		
OH1b	2.006	3.007	-1.001	+0.073	0.952	1.749	167.5
OH1s	4.424	4.265	+0.159	-0.065	0.917		
OH2a	2.510	3.101	-0.591	+0.121	0.892		
OH2b	2.005	3.007	-1.002	+0.071	0.952	1.749	167.5
OH2s	4.424	4.265	+0.159	-0.071	0.917		

This is the peer-reviewed, final accepted version for American Mineralogist, published by the Mineralogical Society of America.
The published version is subject to change. Cite as Authors (Year) Title. American Mineralogist, in press.
DOI: https://doi.org/10.2138/am-2022-8717. http://www.minsocam.org/

Table 6. Comparison of the OH bond intrinsic polarizabilities of the OH bonds in the 'inner' cycle (OHi), those in the 'outer' cycle (OHo) and the non-H-bonded (OHn) in the sassolite model (alpha) with those of a free $B(OH)_3$ unit (alpha_0) as well as their difference (α-α_0), charge (in electron) and bonded OH distance d(OH).

	α (a.u.)	α_0 (a.u.)	α - α_0 (a.u.)	charge	d(OH) (Å)	d(H···O) (Å)
OHi	2.998	4.295	-1.297	-0.094	0.882	1.850
OHo	3.777	4.295	-0.518	-0.154	0.882	1.850
OHn	3.458	4.295	-0.837	-0.025	0.882	1.850

Table 7. Comparison of the OH bond intrinsic polarizabilities between the dimer (α) and corresponding monomers (α_0), together with their difference (α-α_0), the Hirshfeld charge (in electron), the bonded OH distance d(OH), the H-bonded distance d(H···O) and H-bonded valence angle O-H···O for the three dimers modelling kalicinite ($KHCO_3$).

	α (a.u.)	α_0 (a.u.)	α - α_0 (a.u.)	charge	d(OH) (Å)	d(H···O) (Å)	O-H···O (°)
dimer 1							
OH	3.672	4.808	-1.136	-0.139	1.005	1.587	173.0
dimer 2							
OH	4.072	4.808	-0.736	-0.029	1.005	3.385	90.5
dimer 3							
OH	4.206	4.808	-0.602	-0.001	1.005	3.417	99.1
OH	4.800	4.808	-0.008	-0.046	1.005		

This is the peer-reviewed, final accepted version for American Mineralogist, published by the Mineralogical Society of America.
The published version is subject to change. Cite as Authors (Year) Title. American Mineralogist, in press.
DOI: https://doi.org/10.2138/am-2022-8717. http://www.minsocam.org/

Table 8: Comparison of the OH bond intrinsic polarizabilities between the dimer (α) and corresponding monomers (α_0), together with their difference (α-α _0), the Hirshfeld charge (in electron), the bonded OH distance d(OH); the H-bonded distance d(H···O) and H-bonded valence angle O-H···O for the dimer modelling archerite (KH_2PO_4).

dimer	α (a.u.)	α_0 (a.u.)	α - α_0 (a.u.)	charge	d(OH) (Å)	d(H···O) (Å)	O-H···O (°)
OHa	2.028	3.871	-1.843	-0.196	1.066	1.429	177.6
OHb	5.386	4.490	+0.896	-0.053	1.066		
OHc	3.383	3.871	-0.488	-0.026	1.066		
OHd	3.362	4.490	-1.128	+0.012	1.066	3.456	149.7

Table 9. Comparison of the OH bond intrinsic polarizabilities between the dimer (α) and corresponding monomers (α_0), together with their difference (α- α_0), the Hirshfeld charge (in electron), the bonded OH distance d(OH), the H-bonded distance d(H···O), and H-bonded valence angle O-H···O for the four dimers modelling NaH_2PO_4.

dimer 1	α (a.u.)	α_0 (a.u.)	α - α_0 (a.u.)	charge	d(OH) (Å)	d(H···O) (Å)	O-H···O (°)
OH1a	3.156	3.963	-0.807	-0.157	1.041	1.458	167.7
OH1b	4.003	4.074	-0.071	-0.022	1.026		
OH2a	3.156	3.963	-0.807	-0.161	1.041	1.458	167.7
OH2b	4.003	4.074	-0.071	-0.020	1.026		

dimer 2	α (a.u.)	α_0 (a.u.)	α - α_0	charge	d(OH)	d(H···O)	O-H···O

This is the peer-reviewed, final accepted version for American Mineralogist, published by the Mineralogical Society of America.
The published version is subject to change. Cite as Authors (Year) Title. American Mineralogist, in press.
DOI: https://doi.org/10.2138/am-2022-8717. http://www.minsocam.org/

			(a.u.)		(Å)	(Å)	(°)
OH1b	3.704	3.963	-0.259	+0.020	1.041		
OH1a	3.116	4.074	-0.958	-0.123	1.026	1.524	177.6
OH2a	3.957	4.046	-0.089	-0.019	1.001		
OH2b	4.116	4.101	+0.015	-0.049	1.003		

dimer 3	α (a.u.)	α_0 (a.u.)	α - α_0 (a.u.)	charge	d(OH) (Å)	d(H···O) (Å)	O-H···O (°)
OH1b	3.830	4.046	-0.216	-0.025	1.001		
OH1a	2.920	4.101	-1.181	-0.141	1.003	1.589	175.6
OH2a	3.953	3.963	-0.010	-0.006	1.041		
OH2b	3.992	4.074	-0.082	-0.026	1.026		

dimer 4	α (a.u.)	α_0 (a.u.)	α - α_0 (a.u.)	charge	d(OH) (Å)	d(H···O) (Å)	O-H···O (°)
OH1a	2.886	4.046	-1.160	-0.129	1.001	1.644	176.9
OH1b	3.803	4.101	-0.298	-0.015	1.003		
OH2a	3.961	3.963	-0.002	-0.005	1.041		
OH2b	4.078	4.074	+0.004	-0.020	1.026		

This is the peer-reviewed, final accepted version for American Mineralogist, published by the Mineralogical Society of America.
The published version is subject to change. Cite as Authors (Year) Title. American Mineralogist, in press.
DOI: https://doi.org/10.2138/am-2022-8717. http://www.minsocam.org/

636 **Table 10**. Intrinsic polarizability α of the OH bond in CH_3OH and Hirshfeld charge (in

637 electron) as function of the interatomic distance d(H···O) for methanol-dimethylether.

d(H···O) (Å)	α (a.u.)	charge
1.40	4.013	-0.217
1.60	4.038	-0.186
1.80	4.083	-0.160
2.00	4.139	-0.139
2.20	4.201	-0.123
2.40	4.263	-0.111
2.60	4.322	-0.102
2.80	4.377	-0.095
3.00	4.425	-0.090
4.00	4.598	-0.080
5.00	4.691	-0.080
6.00	4.724	-0.080
∞	4.747	-0.080

638

639

This is the peer-reviewed, final accepted version for American Mineralogist, published by the Mineralogical Society of America.
The published version is subject to change. Cite as Authors (Year) Title. American Mineralogist, in press.
DOI: https://doi.org/10.2138/am-2022-8717. http://www.minsocam.org/

640 Figure 1.

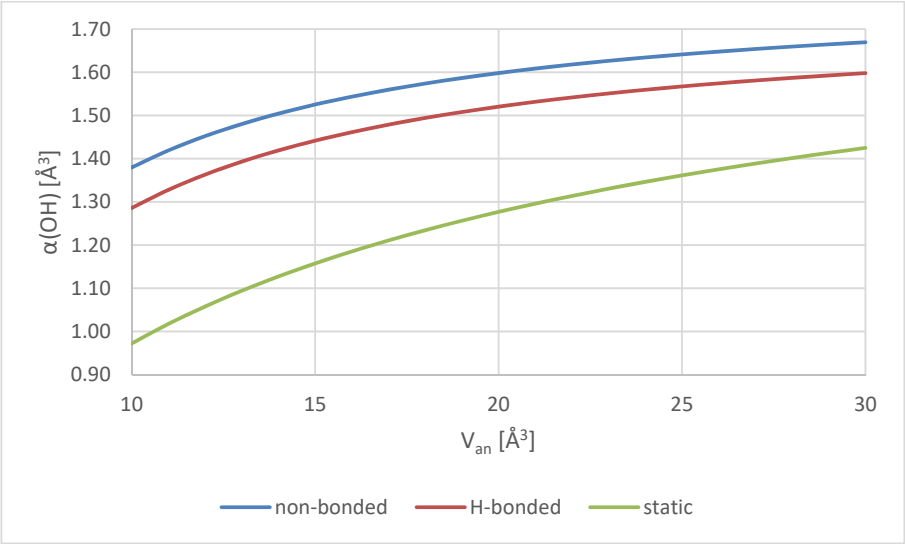

641

642 Figure 2.

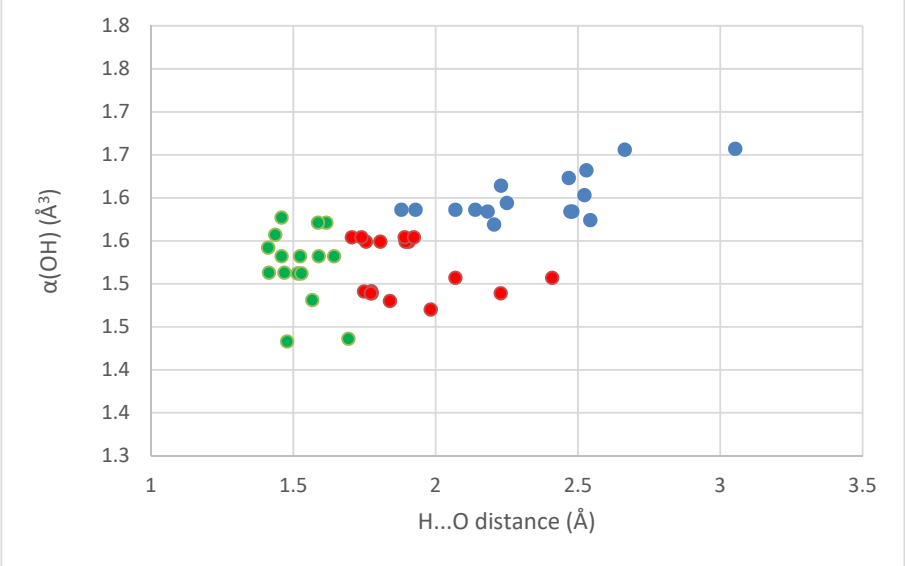

643

644

This is the peer-reviewed, final accepted version for American Mineralogist, published by the Mineralogical Society of America.
The published version is subject to change. Cite as Authors (Year) Title. American Mineralogist, in press.
DOI: https://doi.org/10.2138/am-2022-8717. http://www.minsocam.org/

645 Figure 3.

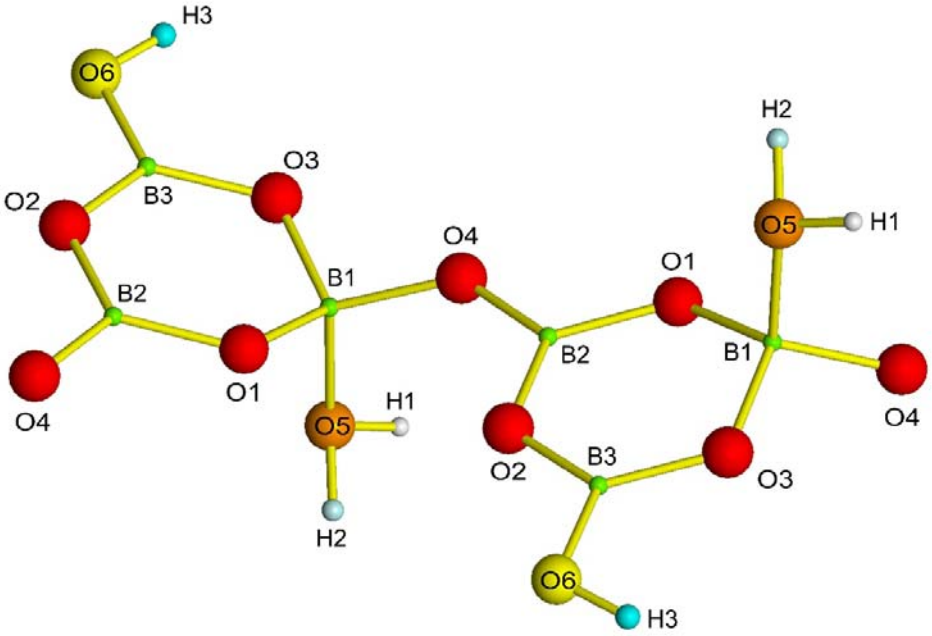

646

647

648

649

650

651

652

653

654

655 Figure 4.

This is the peer-reviewed, final accepted version for American Mineralogist, published by the Mineralogical Society of America.
The published version is subject to change. Cite as Authors (Year) Title. American Mineralogist, in press.
DOI: https://doi.org/10.2138/am-2022-8717. http://www.minsocam.org/

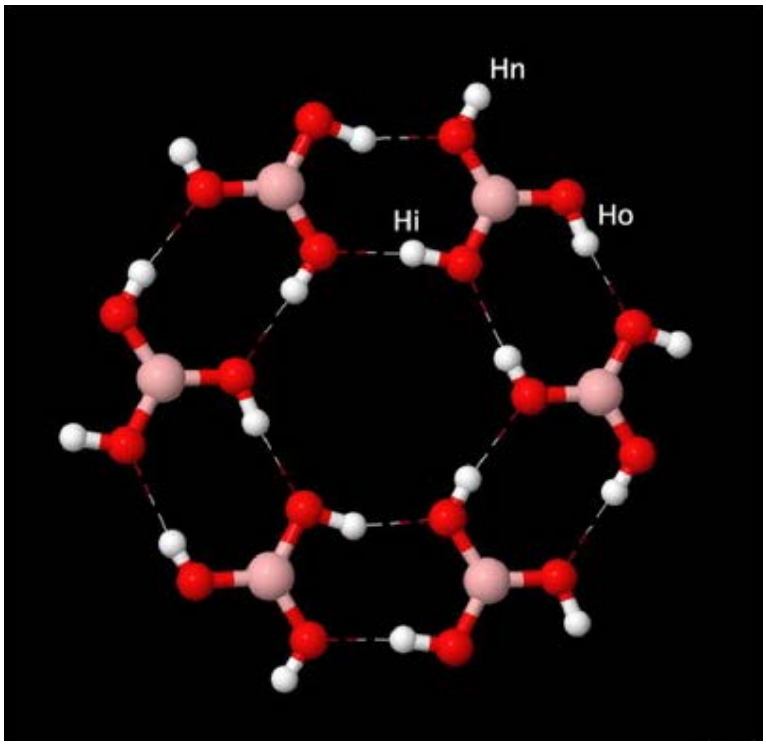

Figure 5.

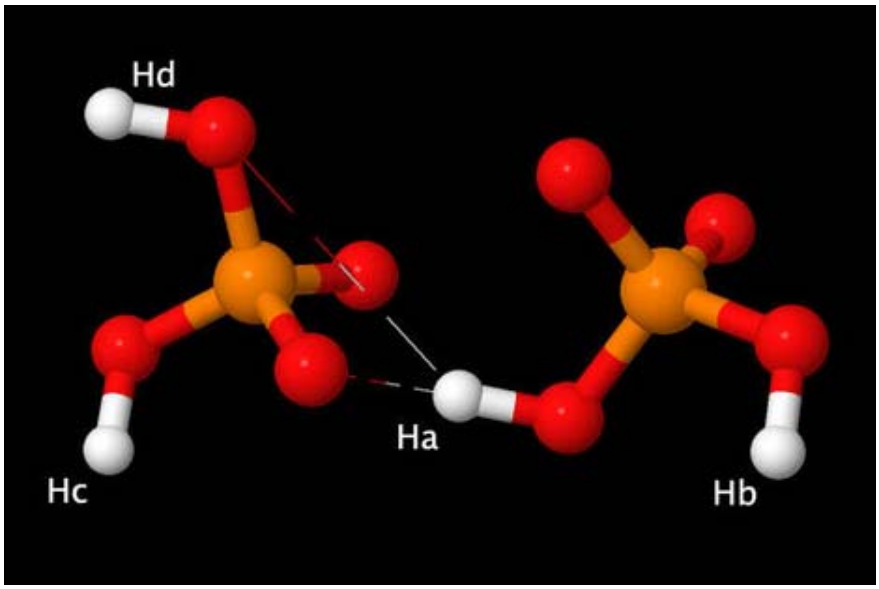

Figure 6.

This is the peer-reviewed, final accepted version for American Mineralogist, published by the Mineralogical Society of America.
The published version is subject to change. Cite as Authors (Year) Title. American Mineralogist, in press.
DOI: https://doi.org/10.2138/am-2022-8717. http://www.minsocam.org/

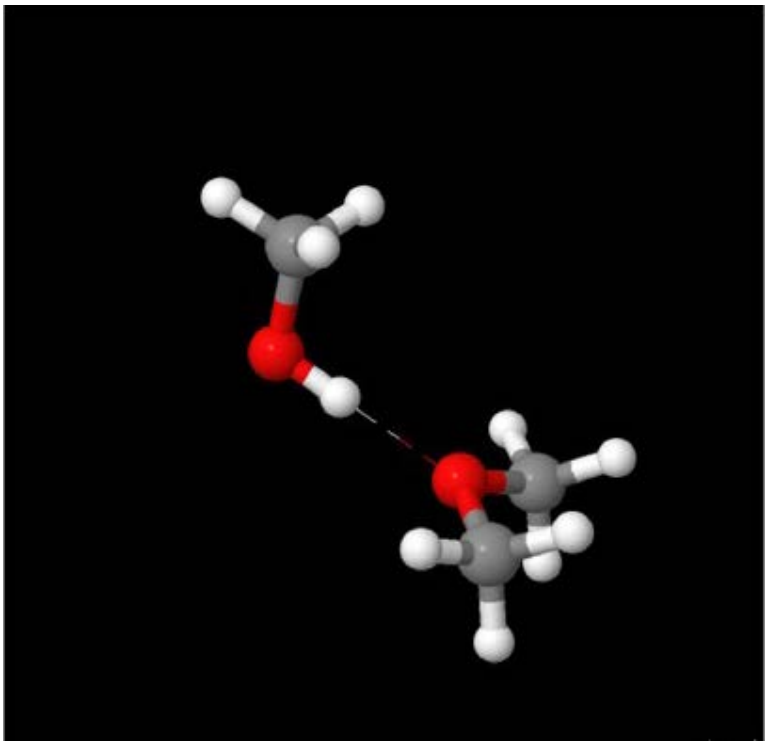

662

663

This is the peer-reviewed, final accepted version for American Mineralogist, published by the Mineralogical Society of America.
The published version is subject to change. Cite as Authors (Year) Title. American Mineralogist, in press.
DOI: https://doi.org/10.2138/am-2022-8717. http://www.minsocam.org/

664 Figure 7.

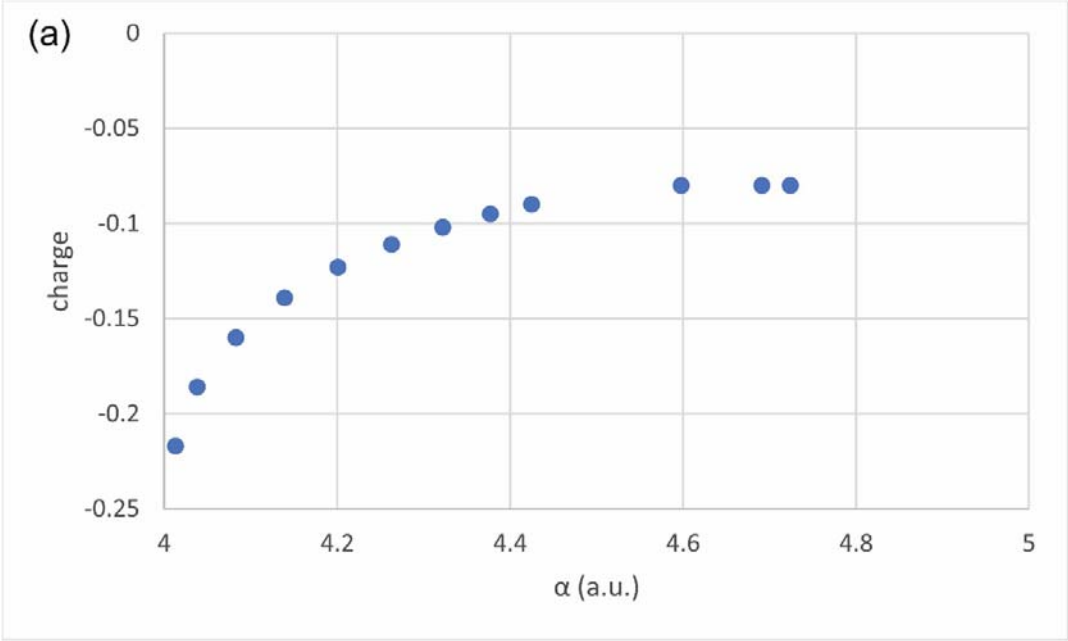

665

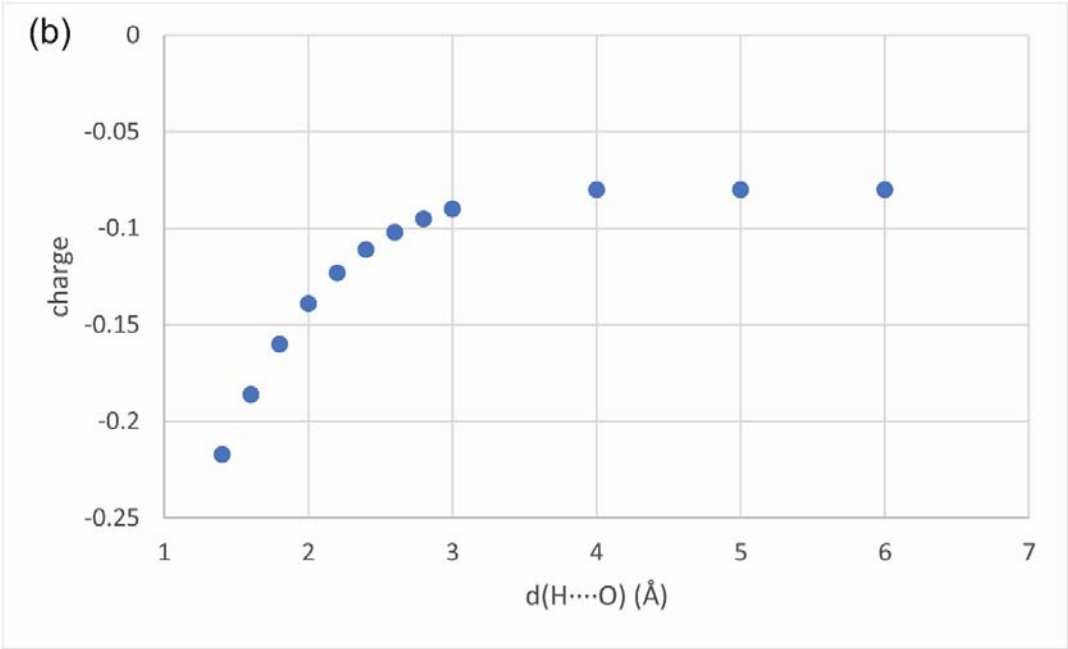

666

667

668

669

This is the peer-reviewed, final accepted version for American Mineralogist, published by the Mineralogical Society of America.
The published version is subject to change. Cite as Authors (Year) Title. American Mineralogist, in press.
DOI: https://doi.org/10.2138/am-2022-8717. http://www.minsocam.org/

Figure 8.